Response of dust emissions in southwestern North America to 21st century trends in climate, CO_2 fertilization, and land use: Implications for air quality

Yang Li[1], Loretta J. Mickley[1], Jed O. Kaplan[2]

[1]John A. Paulson School of Engineering and Applied Sciences, Harvard University, Cambridge, MA, USA

[2]Department of Earth Sciences, The University of Hong Kong, Hong Kong, China

Correspondence to: Yang Li (yangli@seas.harvard.edu)

Abstract. Climate models predict a shift toward warmer and drier environments in southwestern North America over the 21st century. The consequences of climate change for dust mobilization and concentrations are unknown, but could have large implications for human health, given connections between dust inhalation and disease. Here we drive a dynamic vegetation model (LPJ-LMfire) with future scenarios of climate and land use, and link the results to a chemical transport model (GEOS-Chem) to assess the impacts of land cover on dust mobilization and fine dust concentrations (defined as dust particles less than 2.5 microns in diameter) on surface air quality. In the most extreme warming scenario (RCP8.5), we find that surface temperatures in southwestern North America during the season of greatest dust emissions (March, April, and May) warm by 3.3 K and precipitation decreases by nearly 40% by 2100. These conditions lead to vegetation dieback and an increase in dust-producing bare ground. Enhanced CO_2 fertilization, however, offsets the modeled effects of warming temperatures and rainfall deficit on vegetation in some areas of the southwestern United States. Considering all three factors in RCP8.5 scenario, dust concentrations decrease over Arizona and New Mexico in spring by the late 21st century due to greater CO_2 fertilization and a more densely vegetated environment, which inhibits dust mobilization. Along Mexico's northern border, dust concentrations increase as a result of land use intensification. In contrast, when CO_2 fertilization is not considered in the RCP8.5 scenario, vegetation cover declines significantly across most of the domain by 2100, leading to widespread increases in fine dust concentrations, especially in southeastern New Mexico (up to ~2.0 μg m^{-3} relative to the present day) and along the border between New Mexico and Mexico (up to ~2.5 μg m^{-3}). Our results have implications for human health, especially for the health of the indigenous people who make up a large percentage of the population in this region.

1 Introduction

The arid and semi-arid regions of the southwestern United States and northwestern Mexico are characterized by large concentrations of soil-derived dust particles in the lower atmosphere, especially in spring (Hand et al., 2016). By causing respiratory and cardiovascular diseases, fine dust particles – i.e., those particles with diameter less than 2.5 microns – can have negative effects on human health (Tong et al., 2017; Meng and Lu, 2007; Gorris et al., 2018). A key question is to what extent climate change and other factors will influence future dust concentrations in this region, which we define here as southwestern North America. In this study, we use a suite of models to predict the future influence of three factors – climate change, increasing atmospheric CO_2 concentrations, and land use change – on land cover in this region, and assess the consequences for dust mobilization and dust concentrations.

Wind speed and vegetation cover are two key factors that determine soil erodibility and dust emissions. Wind gusts mobilize dust particles from the earth's surface, while vegetation constrains dust emissions by reducing the extent of bare land and preserving soil moisture (Zender et al., 2003). The high temperatures and reduced soil moisture characteristic of drought play an important role in dust mobilization, since loss of vegetative cover during drought increases soil erosion (Archer and Predick, 2008; Bestelmeyer et al., 2018).

Southwestern North America is covered by desert grassland, perennial grassland, savanna, desert scrub, and grassy shrublands or woodlands (McClaran and Van Devender, 1997). In recent decades, a gradual transition from grasslands to shrubland has been observed across much of this region, with increased aridity, atmospheric CO_2 enrichment, and livestock grazing all possibly playing a role in this trend (Bestelmeyer et al., 2018). Future climate change may further prolong this transition, especially since shrubs fare better than grasses under a climate regime characterized by large fluctuations in annual precipitation (Bestelmeyer et al., 2018; Edwards et al., 2019). Climate models predict a warmer and drier environment in southwestern North America through the 21st century, with more frequent and severe drought (Seager and Vecchi, 2010; MacDonald, 2010; Stahle, 2020; Prein et al., 2016; Williams et al., 2020). Such conditions would decrease vegetative cover and allow for greater dust mobilization. On the other hand, elevated CO_2 concentrations in the future atmosphere could increase photosynthesis and decrease transpiration of some vegetation species, allowing for more efficient water use and enhancing growth (Poorter and Perez-Soba, 2002; Polley et al., 2013). Land use practices, e.g., farming and ranching, industrial activities including mining, and urban sprawl, have changed dramatically over the southwestern North America in recent decades, with Arizona and New Mexico showing decreasing cropland area and northern Mexico experiencing increasing pasture area (Figure S1). Future land use practices could also influence the propensity for dust mobilization by disturbing crustal biomass (e.g., Belnap and Gillette, 1998).

Previous studies have investigated the relative importance of climate, CO_2 fertilization, and/or land use in present-day and future dust emissions and concentrations, sometimes with contradictory results. For example, Woodward et al., 2005 predicted a tripling of the global dust burden by 2100 relative to the present day, while other studies suggested a decrease in the global dust burden (e.g., Harrison et al., 2001, Mahowald and Luo, 2003 and Mahowald et al., 2006). These estimates of future dust emissions depended in large part on the choice of model applied, as demonstrated by Tegen et al., 2004.

In southwestern North America, a few recent studies examined statistical relationships between observed present-day dust concentrations and meteorological conditions or leaf area index (LAI). Hand et al., 2016 found that fine dust concentrations in spring in this region correlated with the Pacific Decadal Oscillation (PDO), indicating the importance of large-scale climate patterns in the mobilization and transport of regional fine dust. Tong et al., 2017 further determined that the observed 240% increase in the frequency of windblown dust storms from 1990s to 2000s in the southwestern United States was likely associated with the PDO. Similarly, Achakulwisut et al., 2017 found that the 2002–2015 increase in average March fine dust concentrations in this region was driven by a combination of positive PDO conditions and phase of the El Nino-Southern Oscillation. More recently, Achakulwisut et al., 2018 identified the Standardized Precipitation-Evapotranspiration Index as a useful indicator of present-day dust variability. Applying that metric to an ensemble of future climate projections, these authors predicted increases of 26-46% in fine dust concentrations over the U.S. Southwest in spring by 2100. In contrast, Pu and Ginoux, 2017 found that the frequency of extreme dust days decreases slightly in spring in this region due to reduced extent of bare ground under 21st century climate change.

These regional studies relied mainly on statistical models that relate local and/or large scale meteorological conditions to dust emissions in southwestern North America. Pu and Ginoux, 2017 also considered changing LAI in their model, but these dust-LAI relationships were derived from a relatively sparse dataset, casting some uncertainty on the results (Achakulwisut et al., 2018). In this study, we investigate the effects of climate change, increasing CO_2 fertilization, and future land use practices on vegetation in southwestern North America, and we examine the response of dust mobilization due to these changes in vegetation. With regard to climate, we examine whether a shift to warmer, drier conditions by 2100 enhances dust mobilization in this region by reducing vegetation cover and exposing bare land. To that end, we couple the LPJ-LMfire dynamic vegetation model to the chemical transport model GEOS-Chem to study vegetation dynamics and dust mobilization under different conditions and climate scenarios, allowing consideration of several factors driving future dust mobilization in the southwestern North America. We focus on fine dust particles in springtime (March, April, and May), because it is the season of highest dust concentrations in the southwestern U.S. (Hand et al., 2017). Given the deleterious impacts of airborne dust on human health, our dust projections under different climate scenarios have value for understanding the full array of potential consequences of anthropogenic climate change.

2 Methods

We examine dust mobilization in southwestern North America, here defined as 25°N – 37°N, 100°W – 115°W (Figure 1), during the late-21st century under scenarios of future climate and land use based on two Representative Concentration Pathways (RCPs). RCP4.5 and RCP8.5 capture two possible climate trajectories over the 21st century, beginning in 2006. RCP4.5 represents a scenario of moderate future climate change with gradual reduction in greenhouse gas (GHG) emissions after 2050 and a radiative forcing at 2100 relative to pre-industrial values of +4.5 W m^{-2}, while RCP8.5 represents a more extreme scenario with continued increases in GHGs throughout the 21st century and a radiative forcing of +8.5 W m^{-2} at 2100. For each RCP, we investigate the changes in vegetation for three cases: 1) an all-factor case that includes changes in climate, land use, and CO_2 fertilization; 2) a fixed-CO_2 case that includes changes in only climate and land use; and 3) a fixed-land use case that includes changes in only climate and CO_2 fertilization.

We use LPJ-LMfire, a dynamic global vegetation model, to estimate changes in vegetation under future conditions (Pfeiffer et al., 2013). Meteorology to drive LPJ-LMfire is taken from the Goddard Institute for Space Studies (GISS) climate model (Nazarenko et al., 2015). Using the GEOS-Chem emission component (HEMCO), we then calculate dust emissions based on the LPJ-generated vegetation area index (VAI) for all scenarios. We apply the resulting dust emissions to the global chemical transport model GEOS-Chem to simulate the distribution of fine dust across the southwestern North America.

2.1 GISS Model E

Present-day and future meteorological fields for RCP4.5 and RCP8.5 are simulated by the GISS Model E climate model (Nazarenko et al., 2015), configured for Phase 5 of the Coupled Model Intercomparison Project (CMIP5; https://esgf-node.llnl.gov/search/cmip5/, last accessed on 17 July 2020). The simulations cover the years 1801 to 2100 at a spatial resolution of 2° latitude x 2.5° longitude. Changes in climate in the GISS model are driven by increasing greenhouse gases. In RCP4.5, CO_2 concentrations increase to 550 ppm by 2100; in RCP8.5 the CO_2 increases to 1960 ppm ((Meinshausen et al., 2011).

Under RCP4.5, the GISS model predicts a slight increase of 0.45 K in springtime mean surface temperatures and an increase in mean precipitation by ~17% over the southwestern North America by the 2100 time slice (2095-2099), relative to the present day (2011-2015). In contrast, under RCP8.5, the 5-year mean springtime temperature increases significantly by 3.29 K by 2100 and mean precipitation decreases by ~39%. The spatial distributions of the changes in temperature and precipitation by 2100 under RCP8.5 are presented in the Supplement (Figure S2). In addition, lightning strike densities decrease by ~0.006 strikes km^{-2} d^{-1} over Arizona in RCP4.5, but increase by the same magnitude in this region in RCP8.5 (Li et al., 2020). Lightning strikes play a major role for wildfire ignition in this region, while wildfires may influence landscape succession (e.g., Bodner and Robles, 2017). Finally, future surface wind speeds do not change significantly under RCP4.5, but increase slightly by ~4% across southwestern North America under RCP8.5 by 2100 (not shown). The increasing winds in RCP8.5 will influence the spread of fires in our study, but will not affect the simulated dust fluxes directly, as described in more detail below. Compared to those from other climate models, the GISS projections of climate change in southwestern North America are conservative (Ahlström et al., 2012; Sheffield et al., 2013), implying that our predictions of the impact of climate change on dust mobilization may also be conservative.

In our study, we do not specifically track drought frequency under future climate, as the definition of drought is elusive (Andreadis et al., 2005; Van Loon et al., 2016). Nonetheless, the meteorological conditions predicted in the RCP8.5 scenario for 2100 align with previous studies projecting increased risk of drought in this region (e.g., Williams et al., 2020), and as we shall see, such conditions, in the absence of CO_2 fertilization, result in decreased vegetation and greater dust mobilization.

2.2 LPJ-LMfire

LPJ-LMfire is a fork of the LPJ dynamic vegetation model (Sitch et al., 2003) that includes a process-based representation of fire (Pfeiffer et al., 2013). Input to LPJ-LMfire includes meteorological variables, soil characteristics, land use, and atmospheric CO_2 concentrations, and the model then simulates the corresponding vegetation structure, biogeochemical cycling, and wildfire at a spatial resolution of 0.5° latitude x 0.5° longitude. Here “vegetation structure” refers to vegetation types and the spatial patterns in landscapes.

More specifically, LPJ-LMfire simulates the impacts of photosynthesis, evapotranspiration, and soil water dynamics on vegetation structure and the population densities of different plants functional types (PFTs). The model considers the coupling of different ecosystem processes, such as the interactions between CO_2 fertilization, evapotranspiration, and temperature, as well as the competition among different PFTs for water resources (e.g., precipitation, surface runoff, and drainage). The different PFTs in LPJ-LMfire respond differently to changing CO_2, with CO_2 enrichment preferentially stimulating photosynthesis in woody vegetation and C_3 grasses compared to C_4 grasses (Polley et al., 2013). Wildfire in LPJ-LMfire depends on lightning ignition, and the simulation considers multiday burning, coalescence of fires, and the spread rates of different vegetation types. The effects of changing fire activity on vegetation cover are then taken into account (Pfeiffer et al., 2013; Sitch et al., 2003; Chaste et al., 2019). Li et al., 2020 predicted a ~50% increase in fire-season area burned by 2100 under scenarios of both moderate and intense future climate change over the western United States. However, the effects of changing fire on vegetation cover are insignificant in the grass and bare ground-dominated ecosystems of the desert Southwest, where the low biomass fuels cannot support extensive spread of fires.

For this study we follow Li et al., 2020, in linking meteorology from GISS-E2-R to LPJ-LMfire in order to capture the effects of climate change on vegetation. Meteorological fields from the GISS model include monthly mean surface temperature, diurnal temperature range, total monthly precipitation, number of days in the month with precipitation greater than 0.1 mm, monthly mean total cloud cover fraction, and monthly mean surface wind speed. Monthly mean lightning strike density, calculated using the GISS convective mass flux and the empirical parameterization of Magi, 2015, is also applied to LPJ-LMfire. To downscale the 2° x 2.5° GISS meteorology to finer resolution for LPJ-LMfire, we calculate the 2010-2100 monthly anomalies relative to the average over the 1961-1990 period, and then add these anomalies to an observationally based climatology (Pfeiffer et al., 2013). LPJ-LMfire then simulates the response of natural vegetation to the 21st century trends in these meteorological fields and to increasing CO_2. We apply the same changes in CO_2 concentrations as those applied to the GISS model.

We overlay the changes in natural land cover with future land use scenarios from CMIP5

(LUH; Hurtt et al., 2011; http://tntcat.iiasa.ac.at/RcpDb/, last accessed on 17 July 2020). These scenarios include land used for crops, ranching (rangeland), and urban areas, all of which result in reduction in aboveground biomass, an increase in herbaceous relative to woody plants, and an increase in the extent of bare ground. The present-day land use in the LUH dataset is taken from the HYDE database v3.1 (Goldewijk, 2001; Goldewijk et al., 2010), which in turn is based on array of sources, including satellite observations and government statistics. In RCP8.5, the extent of crop- and rangeland cover increases by ~30% in Mexico but decreases by 10-20% over areas along Mexico's northern border in the U.S. (Hurtt et al., 2011). Only minor changes in land use practices by 2100 are predicted under RCP4.5 (Hurtt et al., 2011).

We perform global simulations with LPJ-LMfire on a 0.5° x 0.5° grid for the two RCPs from 2006-2100, and analyze results over southwestern North America, where dust emissions are especially high. For each RCP we consider the effects of changing climate on land cover, as well as the influence of land use change and CO_2 fertilization. The LPJ-LMfire simulations yield monthly timeseries of the leaf area indices (LAI) and fractional vegetation cover (σ_v) for nine plant functional types (PFTs): tropical broadleaf evergreen, tropical broadleaf raingreen, temperate needleleaf evergreen, temperate broadleaf evergreen, temperate broadleaf summergreen, boreal needleleaf evergreen, and boreal summergreen trees, as well as C_3 and C_4 grasses. We further discuss the LPJ-LMfire present-day land cover in the Supplement.

2.3 VAI calculation

Vegetation constrains dust emissions in two ways: 1) by competing with bare ground as a sink for atmospheric momentum, which results in less drag on erodible soil (Nicholson et al., 1998; Raupach, 1994); and 2) by enhancing soil moisture through plant shade and root systems (Hillel, 1982). Here we implement the dust entrainment and deposition (DEAD) scheme of Zender et al., 2003 to compute a size-segregated dust flux, which includes entrainment thresholds for saltation, moisture inhibition, drag partitioning, and saltation feedback. The scheme assumes that vegetation suppresses dust mobilization by linearly reducing the fraction of bare soil exposed in each grid cell:

$$A_m = (1 - A_l - A_w)(1 - A_s)(1 - A_V) \quad (1),$$

where A_l is the fraction of land covered by lakes, A_w is the fraction covered by wetlands, A_s is the fraction covered by snow, and A_V is the fraction covered by vegetation.

For this study, we use VAI as a metric to represent vegetation because it includes not only leaves but also stems and branches, all of which constrain dust emission. VAI is used to calculate A_V in equation (1) through

$$A_V = \min\,[1.0, \min(VAI, VAI_t)\,/VAI_t] \quad (2),$$

where VAI_t is the threshold for complete suppression of dust emissions, set here to 0.3 m^2 m^{-2} (Zender et al., 2003; Mahowald et al., 1999).

To compute the dust fluxes, we need to convert LAI from LPJ-LMfire to VAI. VAI is generally defined as the sum of LAI plus stem area index (SAI). Assuming immediate removal of all dead leaves, the fractional vegetation cover, σ_v, can be used to represent SAI for the different PFTs (Zeng et al., 2002). Given that the threshold VAI_t for no dust emission is relatively low (0.3 m^2 m^{-2}), leaf area dominates stem area in the suppression of dust mobilization in the model. In areas where LAI is greater than SAI, we therefore assume that SAI does not play a role in controlling dust emissions, and we set LAI equivalent to VAI. We also assume that C_3 and C_4 grasses have zero stem area to avoid overestimating VAI during the winter and early spring when such grasses are dead. Based on the method of Zeng et al., 2002, with modifications, we calculate VAI in each grid cell as

$$VAI = \max\left(\sum_{PFT=1}^{9} LAI, \sum_{PFT=1}^{7} \sigma_v\right) \quad (3)$$

where LAI is for the nine PFTs from LPJ-LMfire, and σ_v is for just seven PFTs, with σ_v for C_3 and C_4 grasses not considered. Of the nine PFTs, temperate needleleaf evergreen, temperate broadleaf evergreen, temperate broadleaf summergreen, and C_3 grasses dominate the region, with temperate needleleaf evergreen having the highest LAI in spring. This mix of vegetation type is consistent with observations (e.g., McClaran and Van Devender, 1997).

2.4 Calculation of dust emissions

Dust emissions are calculated offline in the DEAD dust mobilization module within the Harvard-NASA Emissions Component (HEMCO). We feed into the DEAD module both the VAI generated by LPJ-LMfire and meteorological fields from the Modern-Era Retrospective analysis for Research and Applications (MERRA-2) at a spatial resolution of 0.5° latitude x 0.625° longitude (Gelaro et al., 2017). Dust emission is nonlinear with surface windspeed. Following Ridley et al., 2013, we characterize subgrid-scale surface winds as a Weibull probability distribution, which allows saltation even when the grid-scale wind conditions are below some specified threshold speed. The scheme assumes that the vertical flux of dust is proportional to the horizontal saltation flux, which in turn depends on surface friction velocity and the aerodynamic roughness length Z_0. As recommended by Zender et al., 2003, and consistent with Fairlie et al., 2007 and Ridley et al., 2013, we uniformly set Z_0 to 100 μm across all dust candidate grid cells.

With this model setup, we calculate hourly dust emissions for two five-year time slices for each RCP and condition, covering the present day (2011-2015) and the late-21st century (2095-2099). Dust emissions are generated for four size bins with radii of 0.1 – 1.0 μm, 1.0 – 1.8 μm, 1.8 – 3.0 μm, 3.0 – 6.0 μm. These dust emissions are then applied to GEOS-Chem. Calculated present-day VAI and fine dust emissions are shown in Figure S3, and we compare modeled VAI with that observed in Figures S4 and S5.

2.5 GEOS-Chem

We use the aerosol-only version of the GEOS-Chem chemical transport model (version 12.0.1; http://acmg.seas.harvard.edu/geos/). For computational efficiency, we apply monthly mean oxidants archived from a full-chemistry simulation (Park et al., 2004). To isolate the effect of changing dust mobilization on air quality over the southwestern North America, we use present-day MERRA-2 reanalysis meteorology from NASA/GMAO (Gelaro et al., 2017) for both the present-day and future GEOS-Chem simulations. In other words, we neglect the direct effects of future changes in wind speeds on dust mobilization, allowing us to focus instead on the indirect effects of changing vegetation on dust. For each time slice, we first carry out a global GEOS-Chem simulation at 4° latitude x 5° longitude spatial resolution, and then downscale to 0.5° x 0.625° via grid nesting over the North America domain. In this study, we focus only on dust particles in the finest size bin (i.e., with radii of 0.1 – 1.0 μm), as these are most deleterious to human health. We compare modeled fine dust concentrations over southwestern North America for the present-day against observations from the IMPROVE network in Figures S6-S7.

3 Results

3.1 Spatial shifts in springtime vegetation area index

Figure 1 shows large changes in the spatial distribution of modeled springtime VAI in the southwestern North America for the three cases under both RCPs by 2100. In RCP4.5, the distributions of changes in VAI are similar for the all-factor and fixed-land use cases. Strong enhancements (up to ~2.5 m^2 m^{-2}) extend across much of Arizona, especially in the northwestern corner. The model exhibits moderate VAI increases in most of New Mexico and in the forest regions along the coast of northwestern Mexico. We find decreases in modeled VAI (up to ~ -1.6 $m^2 m^{-2}$) in the southwestern corner of New Mexico, to the east of the coastal forests in Mexico and in the forest regions near the Mexican border connecting with southern Texas. The similarity between the all-factor and fixed land use cases indicates the relatively trivial influence of land use change on vegetation cover in RCP4.5, compared to the effects of climate change and CO_2 fertilization. For the fixed-CO_2 case, western New Mexico and northern Mexico show greater decreases in VAI, indicating how CO_2 fertilization in the other two cases offsets the effects of the warmer and drier climate on vegetation in this region. Figure S8 further illustrates the strong positive impacts that CO_2 fertilization has on VAI.

Compared to RCP4.5, the RCP8.5 scenario shows larger changes in climate, CO_2 concentrations, and land use by 2100 (Figure 1). The net effects of these changes on vegetation are complex. As in RCP4.5, Arizona experiences a strong increase in VAI in the all-factor and fixed-land use cases, but now this increase extends to New Mexico. In contrast to RCP4.5, modeled VAI decreases in the northern Sierra Madre Occidental (Mexico) in the all-factor case for RCP8.5. In the fixed-land use case, however, the VAI decrease in northern Mexico is nearly erased, indicating the role of vegetation/forest degradation caused by land use practices in this area (Figure S9). For the fixed-CO_2 case for RCP8.5, VAI decreases in nearly all of southwestern North America, except the northeastern corner of Arizona and the northwestern corner of New Mexico.

To better understand the changes in VAI, we examine changes in LAI, which represents the major portion of VAI, for the four dominant plant functional types (PFTs) in this region. For example, decreases in LAI in the fixed-CO_2 case under RCP8.5 are dominated by the loss of temperate broadleaf evergreen (TeBE) and temperate broadleaf summergreen (TeBS) (Figure S10).

Temperate needleleaf evergreen (TeNE) shows areas of increase in the northern part and south of Texas in this scenario, while both TeBE and TeBS show increases in northern Arizona and New Mexico. In other areas, TeBS reveals strong decreases, especially in southern Arizona and Mexico. As predicted by previous studies (Bestelmeyer et al., 2018; Edwards et al., 2019), C_3 perennial grasses (C_3gr) in this case decrease across a large swath extending from Arizona through Mexico, showing the impacts of warmer temperatures and reduced precipitation, as well as (for Mexico) land use change. Increased fire activity also likely plays a role in the simulated decreases of forest cover and C_3 grasses for RCP8.5 in southern Arizona, where fires together with drought may have affected landscape succession (Williams et al., 2013; Bodner and Robles, 2017). We also investigate trends in LAI for different months in spring from the present day to 2100. We find that the greatest percentage decreases in TeBS and C_3 grasses occur in May, consistent with the largest decreases in precipitation in that month (not shown).

In summary, we find that the warmer and drier conditions of the future climate strongly reduce vegetation cover by 2100, especially in RCP8.5. In addition, CO_2 fertilization and land use practices further modify future vegetation, but in opposite ways, as illustrated by Figure S8. Under a warmer climate, higher CO_2 concentrations facilitate vegetation growth everywhere in the southwestern North America, with larger VAI increases occurring over Arizona and New Mexico. Combined changes in land use are greater under RCP8.5 than RCP4.5, with large increases in RCP8.5 across Mexico but only modest changes in Arizona, New Mexico, and Texas (Figure S9). The increases in Mexico result in the fragmentation of forested landscapes and decrease VAI, especially in coastal forest regions and along the border with the United States.

3.2 Spatial variations in spring fine dust emissions

Unlike the widespread changes in VAI, future changes in fine dust emissions are concentrated in a few arid areas, including: 1) the border regions connecting Arizona, New Mexico, and northern Mexico (ANM border), 2) eastern New Mexico, and 3) western Texas (Figure 2). In RCP4.5, slight increases in fine dust emission (up to ~0.3 kg m^{-2} mon^{-1}) are simulated in the ANM border in all the three cases. In contrast, fine dust emissions decrease by up to ~ -1.0 kg m^{-2} mon^{-1} in eastern New Mexico and western Texas in RCP4.5 due to warmer temperatures and increasing VAI. Consistent with the modest changes in VAI (Figure 1), the three cases in RCP4.5 do not exhibit large differences, with only the fixed-CO_2 case showing slightly greater increases in dust emissions along the ANM border and in western Texas. In RCP8.5 in the all-factor case, spring fine dust emissions increase slightly by up to ~ 0.4 kg m^{-2} mon^{-1} along the ANM border, but decrease more strongly in western Texas by up to ~ -1.4 kg m^{-2} mon^{-1} (Figure 2). In contrast, with fixed CO_2 the sign of the change in dust emissions reverses, with significant emissions increases along the ANM border and in New Mexico. The area with decreasing emissions in western Texas also shrinks in the fixed CO_2 case. These trends occur due to the climate stresses, e.g., warmer temperatures and decreased precipitation, that impair the growth of temperature broadleaf trees and C_3 grasses. In this case, such stresses are not offset by CO_2 fertilization (Figure S10).

Figure 3 shows more vividly the opposing roles of CO_2 fertilization and projected land use change in southwestern North America. In RCP8.5, changing CO_2 fertilization alone promotes vegetation growth and dramatically reduces dust mobilization by up to ~ -1.2 kg m^{-2} mon^{-1}. Figure 3 also reveals that land use trends are a major driver of increased dust emissions along the ANM border and western Texas in RCP8.5, as crop- and rangelands expand in this region and temperature broadleaf trees decline (Hurtt et al., 2011). Similarly, the expansion of rangelands in northern Mexico in RCP8.5 reduces natural vegetation cover there (Hurtt et al., 2011), contributing to the increase of fine dust emissions by up to ~0.7 kg m^{-2} mon^{-1}.

3.3 Spring fine dust concentrations under the high emission scenario

Our simulations suggest that fine dust emissions will increase across arid areas in southwestern North America under RCP8.5, but only if CO_2 fertilization is of minimal importance (Figure 2). To place an upper bound on future concentrations of fine dust in this region, we apply only the fixed-CO_2 emissions to GEOS-Chem at the horizontal resolution of 0.5° x 0.625°. Given the large uncertainty in the sensitivity of vegetation to changing atmospheric CO_2 concentrations (Smith et al., 2016), we argue that this approach is justified.

Results from GEOS-Chem in the fixed-CO_2 case for RCP8.5 show that the concentrations of spring fine dust are significantly enhanced in the southeastern half of New Mexico and along the ANM border, with increases up to ~2.5 $\mu g\ m^{-3}$ (Figure 4). The model also yields elevated dust concentrations over nearly the entire extent of our study region by 2100. As Figure 3 implies, land use along the ANM border contributes to the increased dust emissions in that area, by up to ~0.7 $kg\ m^{-2}\ mon^{-1}$. Climate change impacts on natural vegetation, however, account for the bulk of the modeled increases in dust emissions in this scenario, by as much as ~1.2 $kg\ m^{-2}\ mon^{-1}$ (Figure 2). The modeled wind fields, which are the same in all scenarios, transport the dust from source regions, leading to the enhanced concentrations across much of the domain, as seen in Figure 4. We find that dust concentrations decrease only in a limited area in western Texas due to decreased pasture (Figures 3 and S9).

4 Discussion

We apply a coupled modeling approach to investigate the impact of future changes in climate, CO_2 fertilization, and land use on dust mobilization and fine dust concentration in southwestern North America by the end of the 21st century. Table 1 summarizes our findings for the two RCP scenarios and three conditions – all-factor, fixed CO_2, and fixed land use – in spring, when dust concentrations are greatest. We find that in the RCP8.5 fixed-CO_2 scenario, in which the effects of CO_2 fertilization are neglected, VAI decreases by 26% across the region due mainly to warmer temperatures and drier conditions, yielding an increase of 58% in fine dust emission averaged over the southwestern North America. In addition, we find that the increase in fine dust emission in northern Mexico is mainly driven by the increases in the extent of cropland and pasture cover in this area, signifying the crucial role of land use practices in modifying dust mobilization.

Our findings of decreasing VAI with future climate change are consistent with observed trends in vegetation during recent droughts in this region. For example, Breshears et al., 2005 documented large-scale die-off of overstory trees across southwestern North America in 2002-2003 in response to short-term drought accompanied by bark beetle infestations. Similarly, during a multi-year (2004-2014) drought in southern Arizona, Bodner and Robles, 2017 found that the spatial extent of both C_4 grass cover and shrub cover decreased in the southeastern part of that state.

The 58% increase predicted in this study in fixed-CO_2 RCP8.5 scenario is larger than the 26-46% future increases in fine dust for this region predicted by the statistical model of Achakulwisut et al., 2018. That study relied solely on predictions of future regional-scale meteorology and did not take into account the change in vegetation, as we do here. In contrast, the statistical model of Pu and Ginoux, 2017 estimated a 2% decrease in the springtime frequency of extreme dust events in the Southwest U.S., driven mainly by reductions in bare ground fraction and wind speed. Like Pu and Ginoux, 2017, we also find that dust emissions decrease across a broad region of the Southwest when CO_2 fertilization is taken into account, as shown in Figure 2. Pu and Ginoux, 2017 relied on limited data for capturing the sensitivity of dust event frequency to land cover in this region, and neither that study nor Achakulwisut et al., 2018 considered changes in land use, as do here. The direct effects of changing wind speed on dust mobilization, however, are not included in our study, but could be tested in future work.

We further find that consideration of CO_2 fertilization can mitigate the effects of changing climate and land use on dust concentrations in southwestern North America. The all-factor and fixed-land use simulations both yield decreases of ~20% in mean dust emissions compared to the early 21st century. In the IPCC projections, CO_2 reaches ~550 ppm by 2100 under RCP4.5 and ~1960 ppm under RCP8.5 (Meinshausen et al., 2011). Correspondingly, in the RCP4.5 scenario for 2100, CO_2 fertilization enhances VAI by 30% in the all-factor case compared to the fixed-CO_2 case (1.07 m^2m^{-2} vs. 0.79 m^2m^{-2}); in RCP 8.5, the 2100 enhancement is 64% (1.11 m^2m^{-2} vs. 0.55 m^2m^{-2}), as shown in Table 1. These enhancements further decrease fine dust emissions by 21% under RCP4.5 and 78% under RCP8.5, compared to the present day. Except along the ANM border and a few other areas, trends in land use have only minor impacts on dust mobilization under the two RCPs in southwestern North America.

In summary, we find that as atmospheric CO_2 levels rise vegetation growth is enhanced and dust mobilization decreases, offsetting the impacts of warmer temperatures and reduced rainfall, at least in some areas. These results are consistent with evidence that CO_2 fertilization is already occurring in arid or semiarid environments like southwestern North America (Donohue et al., 2013; Haverd et al., 2020). In such environments, water availability is the dominant constraint on vegetation growth, and the recent increases in atmospheric CO_2 may have reduced stomatal conductance and limited evaporative water loss. The effects of CO_2 fertilization on vegetation growth are uncertain, however, and may be attenuated by the limited supply of nitrogen and phosphorus in soil (Wieder et al., 2015). These nutritional constraints vary greatly among different PFTs (Shaw et al., 2002; Nadelhoffer et al., 1999).

Understanding the drivers in historic dust trends has sometimes been challenging (Mahowald and Luo, 2003; Mahowald et al., 2002), making it difficult to validate dust mobilization models. A further drawback of our approach is that the LPJ-LMfire model is driven by meteorological fields from just one climate model, GISS-E2-R. Given that the GISS model yields a conservative prediction of climate change in the southwestern North America compared to other models (Ahlström et al., 2012; Sheffield et al., 2013), our predictions of the impact of climate change on dust mobilization may also be conservative. Other uncertainties in our study can be traced to the dust simulation. The different vegetation types in our model are quantified as fractions of gridcells, which have relatively large spatial dimensions of ~50 km × 60 km. This means the model cannot capture the spatial heterogeneity of land cover, and the aerodynamic sheltering effects of vegetation on wind erosion are neglected, as they are in most 3-D global model studies. Such sheltering could play a large role in dust mobilization (e.g., Liu et al., 1990). New methods involving satellite observations of surface albedo promise to improve understanding of the effects of aerodynamic sheltering on dust mobilization, at least for the present-day (Chappell and Webb, 2016; Webb and Pierre, 2018). Implementation of aerodynamic sheltering in simulations of future climate regimes would need to account for fine-scale spatial distributions of vegetation. In addition, as recommended by Zender et al., 2003, we apply a globally uniform surface roughness Z_0 in the model, which means that the impact of changing vegetation conditions on friction velocity is not taken into account. Future work could address this weakness by varying friction velocity according to vegetation type. Finally, our study focuses only on the effect of changing vegetation on dust mobilization and does not take into account how changing windspeeds or drier soils in the future atmosphere may more directly influence dust. Given the slight increase in monthly mean winds in RCP8.5 by 2100, future dust emissions in this scenario could be underestimated.

Within these limitations, our study quantifies the potential impacts of changing land cover and land use practices on dust mobilization and fine dust concentration over the coming century in southwestern North America. Our work builds on previous studies focused on future dust in this region by (1) more accurately capturing the transport of dust from source regions with a dynamical 3-D model, (2) considering results with and without CO_2 enhancement, and (3) including the impact of land use trends. Given the many uncertainties, it is challenging to gauge which of the three factors investigated here – climate impacts on vegetation, CO_2 fertilization, or land use change – will play the dominant role in driving future changes in dust emissions and concentrations. This study thus brackets a range of possible dust scenarios for the southwestern North America, with the simulation without CO_2 fertilization placing an upper bound on dust emissions. In the absence of increased CO_2 fertilization, our work suggests that vegetated cover will contract in response to the warmer, drier climate, exposing bared ground and significantly increasing dust concentrations by 2100. In this way, dust enhancement could impose a potentially large climate penalty on $PM_{2.5}$ air quality, with consequences for human health across much of southwestern North America.

Our finding of the potential for an increased dust burden in the future atmosphere has special relevance for environmental justice in this region, where much of the current population is of Native American and/or Latino descent. For example, in New Mexico, 10% of the population is Native American and 50% identifies as either Hispanic or Latino. By some measures, New

Mexico has also one of highest poverty rates of the United States (https://www.census.gov /quickfacts/NM, last accessed on August 20, 2020).

Code and data availability

GEOS-Chem model codes can be obtained at http://acmg.seas.harvard.edu/geos. LPJ-LMfire model codes can be obtained at https://github.com/ARVE-Research/LPJ-LMfire. IMPROVE datasets are available online at http://vista.cira.colostate.edu/improve. Any additional information related to this paper may be requested from the authors.

Author contributions

Y.L. conceived and designed the study, performed the GEOS-Chem simulations, analyzed the data, and wrote the manuscript, with contributions from all coauthors. J.O.K. performed the LPJ-LMfire simulations.

Competing interests

The authors declare that they have no competing interest.

Acknowledgments

This research was developed under Assistance Agreements 83587501 and 83587201 awarded by the U.S. Environmental Protection Agency (EPA). It has not been formally reviewed by the EPA. The views expressed in this document are solely those of the authors and do not necessarily reflect those of the EPA. We thank all of the data providers of the datasets used in this study. PM data was provided by the Interagency Monitoring of Protected Visual Environments (IMPROVE; available online at http://vista.cira.colostate.edu/improve). IMPROVE is a collaborative association of state, tribal, and federal agencies, and international partners. U.S. Environmental Protection Agency is the primary funding source, with contracting and research support from the National Park Service. JOK is grateful for access to computing resources provided by the School of Geography and the Environment, University of Oxford. The Air Quality Group at the University of California, Davis is the central analytical laboratory, with ion analysis provided by the Research Triangle Institute, and carbon analysis provided by the Desert Research Institute. We acknowledge the World Climate Research Programme's Working Group on Coupled Modelling, which is responsible for CMIP, and we thank the group of NASA Goddard Institute for Space Studies for producing and making available their GISS-E2-R climate model output. For CMIP the U.S. Department of Energy's Program for Climate Model Diagnosis and Intercomparison provides coordinating support and led development of software infrastructure in partnership with the Global Organization for Earth System Science Portals. The GISS-E2-R dataset were downloaded from https://cmip.llnl.gov/cmip5/. We thank the Land-use Harmonization team for producing the harmonized set of land-use scenarios and making available the dataset online at http://tntcat.iiasa.ac.at/RcpDb/.

References

Achakulwisut, P., Shen, L., and Mickley, L. J.: What controls springtime fine dust variability in the western United States? Investigating the 2002–2015 increase in fine dust in the US Southwest, Journal of Geophysical Research: Atmospheres, 122, 2017.

Achakulwisut, P., Mickley, L., and Anenberg, S.: Drought-sensitivity of fine dust in the US Southwest: Implications for air quality and public health under future climate change, Environmental Research Letters, 13, 054025, 2018.

Ahlström, A., Schurgers, G., Arneth, A., and Smith, B.: Robustness and uncertainty in terrestrial ecosystem carbon response to CMIP5 climate change projections, Environmental Research Letters, 7, 044008, 2012.

Andreadis, K. M., Clark, E. A., Wood, A. W., Hamlet, A. F., and Lettenmaier, D. P.: Twentieth-century drought in the conterminous United States, Journal of Hydrometeorology, 6, 985-1001, 2005.

Archer, S. R., and Predick, K. I.: Climate change and ecosystems of the southwestern United States, Rangelands, 30, 23-28, 2008.

Belnap, J., and Gillette, D. A.: Vulnerability of desert biological soil crusts to wind erosion: the influences of crust development, soil texture, and disturbance, Journal of arid environments, 39, 133-142, 1998.

Bestelmeyer, B. T., Peters, D. P. C., Archer, S. R., Browning, D. M., Okin, G. S., Schooley, R. L., and Webb, N. P.: The Grassland–Shrubland Regime Shift in the Southwestern United States: Misconceptions and Their Implications for Management, BioScience, 68, 678-690, 10.1093/biosci/biy065, 2018.

Bodner, G. S., and Robles, M. D.: Enduring a decade of drought: Patterns and drivers of vegetation change in a semi-arid grassland, Journal of Arid Environments, 136, 1-14, 2017.

Breshears, D. D., Cobb, N. S., Rich, P. M., Price, K. P., Allen, C. D., Balice, R. G., Romme, W. H., Kastens, J. H., Floyd, M. L., Belnap, J., Anderson, J. J., Myers, O. B., and Meyer, C. W.: Regional vegetation die-off in response to global-change-type drought, Proc Natl Acad Sci U S A, 102, 15144-15148, 10.1073/pnas.0505734102, 2005.

Chappell, A., and Webb, N. P.: Using albedo to reform wind erosion modelling, mapping and monitoring, Aeolian Research, 23, 63-78, 2016.

Chaste, E., Girardin, M. P., Kaplan, J. O., Bergeron, Y., and Hély, C.: Increases in heat-induced tree mortality could drive reductions of biomass resources in Canada’s managed boreal forest, Landscape Ecology, 34, 403-426, 2019.

Donohue, R. J., Roderick, M. L., McVicar, T. R., and Farquhar, G. D.: Impact of CO2 fertilization on maximum foliage cover across the globe's warm, arid environments, Geophysical Research Letters, 40, 3031-3035, 2013.

Edwards, B., Webb, N., Brown, D., Elias, E., Peck, D., Pierson, F., Williams, C., and Herrick, J.: Climate change impacts on wind and water erosion on US rangelands, Journal of Soil and Water Conservation, 74, 405-418, 2019.

Fairlie, T. D., Jacob, D. J., and Park, R. J.: The impact of transpacific transport of mineral dust in the United States, Atmos Environ, 41, 1251-1266, 2007.

Gelaro, R., McCarty, W., Suarez, M. J., Todling, R., Molod, A., Takacs, L., Randles, C., Darmenov, A., Bosilovich, M. G., Reichle, R., Wargan, K., Coy, L., Cullather, R., Draper, C., Akella, S., Buchard, V., Conaty, A., da Silva, A., Gu, W., Kim, G. K., Koster, R., Lucchesi, R., Merkova, D., Nielsen, J. E., Partyka, G., Pawson, S., Putman, W., Rienecker, M., Schubert, S.

D., Sienkiewicz, M., and Zhao, B.: The Modern-Era Retrospective Analysis for Research and Applications, Version 2 (MERRA-2), J Clim, Volume 30, 5419-5454, 10.1175/JCLI-D-16-0758.1, 2017.
Goldewijk, K. K.: Estimating global land use change over the past 300 years: the HYDE database, Global biogeochemical cycles, 15, 417-433, 2001.
Goldewijk, K. K., Beusen, A., van Drecht, G., and de Vos, M.: The HYDE 3.1 spatially explicit database of human-induced global land-use change over the past 12,000 yearsgeb_587, 2010.
Gorris, M. E., Cat, L. A., Zender, C. S., Treseder, K. K., and Randerson, J. T.: Coccidioidomycosis Dynamics in Relation to Climate in the Southwestern United States, Geohealth, 2, 6-24, 10.1002/2017GH000095, 2018.
Hand, J., White, W., Gebhart, K., Hyslop, N., Gill, T., and Schichtel, B.: Earlier onset of the spring fine dust season in the southwestern United States, Geophysical Research Letters, 43, 4001-4009, 2016.
Hand, J., Gill, T., and Schichtel, B.: Spatial and seasonal variability in fine mineral dust and coarse aerosol mass at remote sites across the United States, Journal of Geophysical Research: Atmospheres, 122, 3080-3097, 2017.
Harrison, S. P., Kohfeld, K. E., Roelandt, C., and Claquin, T.: The role of dust in climate changes today, at the last glacial maximum and in the future, Earth-Science Reviews, 54, 43-80, 2001.
Haverd, V., Smith, B., Canadell, J. G., Cuntz, M., Mikaloff-Fletcher, S., Farquhar, G., Woodgate, W., Briggs, P. R., and Trudinger, C. M.: Higher than expected CO2 fertilization inferred from leaf to global observations, Global change biology, 26, 2390-2402, 2020.
Hillel, D.: Introduction to soil physics.,(Academic Press: San Diego, CA), Introduction to soil physics. Academic Press, San Diego, CA., -, 1982.
Hurtt, G. C., Chini, L. P., Frolking, S., Betts, R., Feddema, J., Fischer, G., Fisk, J., Hibbard, K., Houghton, R., and Janetos, A.: Harmonization of land-use scenarios for the period 1500–2100: 600 years of global gridded annual land-use transitions, wood harvest, and resulting secondary lands, Climatic change, 109, 117, 2011.
Li, Y., Mickley, L. J., Liu, P., and Kaplan, J. O.: Trends and spatial shifts in lightning fires and smoke concentrations in response to 21st century climate over the national forests and parks of the western United States, Atmospheric Chemistry and Physics, 20, 8827-8838, 10.5194/acp-20-8827-2020, 2020.
Liu, S.-J., Wu, H.-I., Lytton, R. L., and Sharpe, P. J.: Aerodynamic sheltering effects of vegetative arrays on wind erosion: A numerical approach, Journal of environmental management, 30, 281-294, 1990.
MacDonald, G. M.: Climate Change and water in Southwestern North America special feature: water, climate change, and sustainability in the southwest, Proc Natl Acad Sci U S A, 107, 21256-21262, 10.1073/pnas.0909651107, 2010.
Magi, B. I.: Global lightning parameterization from CMIP5 climate model output, Journal of Atmospheric and Oceanic Technology, 32, 434-452, 2015.
Mahowald, N., Kohfeld, K., Hansson, M., Balkanski, Y., Harrison, S. P., Prentice, I. C., Schulz, M., and Rodhe, H.: Dust sources and deposition during the last glacial maximum and current climate: A comparison of model results with paleodata from ice cores and marine sediments, Journal of Geophysical Research: Atmospheres, 104, 15895-15916, 1999.

Mahowald, N. M., Zender, C. S., Luo, C., Savoie, D., Torres, O., and Del Corral, J.: Understanding the 30-year Barbados desert dust record, Journal of Geophysical Research: Atmospheres, 107, AAC 7-1-AAC 7-16, 2002.

Mahowald, N. M., and Luo, C.: A less dusty future?, Geophysical Research Letters, 30, 2003.

Mahowald, N. M., Muhs, D. R., Levis, S., Rasch, P. J., Yoshioka, M., Zender, C. S., and Luo, C.: Change in atmospheric mineral aerosols in response to climate: Last glacial period, preindustrial, modern, and doubled carbon dioxide climates, Journal of Geophysical Research: Atmospheres, 111, 2006.

McClaran, M. P., and Van Devender, T. R.: The desert grassland, University of Arizona Press, 1997.

Meinshausen, M., Smith, S. J., Calvin, K., Daniel, J. S., Kainuma, M., Lamarque, J.-F., Matsumoto, K., Montzka, S., Raper, S., and Riahi, K.: The RCP greenhouse gas concentrations and their extensions from 1765 to 2300, Climatic change, 109, 213, 2011.

Meng, Z., and Lu, B.: Dust events as a risk factor for daily hospitalization for respiratory and cardiovascular diseases in Minqin, China, Atmos Environ, 41, 7048-7058, 2007.

Nadelhoffer, K. J., Emmett, B. A., Gundersen, P., Kjønaas, O. J., Koopmans, C. J., Schleppi, P., Tietema, A., and Wright, R. F.: Nitrogen deposition makes a minor contribution to carbon sequestration in temperate forests, Nature, 398, 145, 1999.

Nazarenko, L., Schmidt, G., Miller, R., Tausnev, N., Kelley, M., Ruedy, R., Russell, G., Aleinov, I., Bauer, M., and Bauer, S.: Future climate change under RCP emission scenarios with GISS ModelE2, Journal of Advances in Modeling Earth Systems, 7, 244-267, 2015.

Nicholson, S. E., Tucker, C. J., and Ba, M.: Desertification, drought, and surface vegetation: An example from the West African Sahel, Bulletin of the American Meteorological Society, 79, 815-830, 1998.

Park, R. J., Jacob, D. J., Field, B. D., Yantosca, R. M., and Chin, M.: Natural and transboundary pollution influences on sulfate-nitrate-ammonium aerosols in the United States: Implications for policy, Journal of Geophysical Research: Atmospheres, 109, 2004.

Pfeiffer, M., Spessa, A., and Kaplan, J. O.: A model for global biomass burning in preindustrial time: LPJ-LMfire (v1. 0), Geoscientific Model Development, 6, 643-685, 2013.

Polley, H. W., Briske, D. D., Morgan, J. A., Wolter, K., Bailey, D. W., and Brown, J. R.: Climate change and North American rangelands: trends, projections, and implications, Rangeland Ecology & Management, 66, 493-511, 2013.

Poorter, H., and Perez-Soba, M.: Plant growth at elevated CO2, Encyclopedia of global environmental change, 2, 489-496, 2002.

Prein, A. F., Holland, G. J., Rasmussen, R. M., Clark, M. P., and Tye, M. R.: Running dry: The US Southwest's drift into a drier climate state, Geophysical Research Letters, 43, 1272-1279, 2016.

Pu, B., and Ginoux, P.: Projection of American dustiness in the late 21(st) century due to climate change, Sci Rep, 7, 5553, 10.1038/s41598-017-05431-9, 2017.

Raupach, M.: Simplified expressions for vegetation roughness length and zero-plane displacement as functions of canopy height and area index, Boundary-Layer Meteorol, 71, 211-216, 1994.

Ridley, D. A., Heald, C. L., Pierce, J., and Evans, M.: Toward resolution-independent dust emissions in global models: Impacts on the seasonal and spatial distribution of dust, Geophysical Research Letters, 40, 2873-2877, 2013.

Seager, R., and Vecchi, G. A.: Greenhouse warming and the 21st century hydroclimate of southwestern North America, Proc Natl Acad Sci U S A, 107, 21277-21282, 10.1073/pnas.0910856107, 2010.
Shaw, M. R., Zavaleta, E. S., Chiariello, N. R., Cleland, E. E., Mooney, H. A., and Field, C. B.: Grassland responses to global environmental changes suppressed by elevated CO2, Science, 298, 1987-1990, 10.1126/science.1075312, 2002.
Sheffield, J., Barrett, A. P., Colle, B., Nelun Fernando, D., Fu, R., Geil, K. L., Hu, Q., Kinter, J., Kumar, S., and Langenbrunner, B.: North American climate in CMIP5 experiments. Part I: Evaluation of historical simulations of continental and regional climatology, Journal of Climate, 26, 9209-9245, 2013.
Sitch, S., Smith, B., Prentice, I. C., Arneth, A., Bondeau, A., Cramer, W., Kaplan, J. O., Levis, S., Lucht, W., Sykes, M. T., Thonicke, K., and Venevsky, S.: Evaluation of ecosystem dynamics, plant geography and terrestrial carbon cycling in the LPJ dynamic global vegetation model, Global Change Biology, 9, 161-185, 10.1046/j.1365-2486.2003.00569.x, 2003.
Smith, W. K., Reed, S. C., Cleveland, C. C., Ballantyne, A. P., Anderegg, W. R., Wieder, W. R., Liu, Y. Y., and Running, S. W.: Large divergence of satellite and Earth system model estimates of global terrestrial CO 2 fertilization, Nature Climate Change, 6, 306, 2016.
Stahle, D. W.: Anthropogenic megadrought, Science, 368, 238-239, 10.1126/science.abb6902, 2020.
Tegen, I., Werner, M., Harrison, S., and Kohfeld, K.: Relative importance of climate and land use in determining present and future global soil dust emission, Geophysical Research Letters, 31, 2004.
Tong, D. Q., Wang, J. X. L., Gill, T. E., Lei, H., and Wang, B.: Intensified dust storm activity and Valley fever infection in the southwestern United States, Geophys Res Lett, 44, 4304-4312, 10.1002/2017GL073524, 2017.
Van Loon, A. F., Stahl, K., Di Baldassarre, G., Clark, J., Rangecroft, S., Wanders, N., Gleeson, T., Van Dijk, A. I., Tallaksen, L. M., and Hannaford, J.: Drought in a human-modified world: reframing drought definitions, understanding, and analysis approaches, 2016.
Webb, N. P., and Pierre, C.: Quantifying anthropogenic dust emissions, Earth's Future, 6, 286-295, 2018.
Wieder, W. R., Cleveland, C. C., Smith, W. K., and Todd-Brown, K.: Future productivity and carbon storage limited by terrestrial nutrient availability, Nature Geoscience, 8, 441, 2015.
Williams, A. P., Allen, C. D., Macalady, A. K., Griffin, D., Woodhouse, C. A., Meko, D. M., Swetnam, T. W., Rauscher, S. A., Seager, R., and Grissino-Mayer, H. D.: Temperature as a potent driver of regional forest drought stress and tree mortality, Nature climate change, 3, 292-297, 2013.
Williams, A. P., Cook, E. R., Smerdon, J. E., Cook, B. I., Abatzoglou, J. T., Bolles, K., Baek, S. H., Badger, A. M., and Livneh, B.: Large contribution from anthropogenic warming to an emerging North American megadrought, Science, 368, 314-318, 2020.
Woodward, S., Roberts, D., and Betts, R.: A simulation of the effect of climate change–induced desertification on mineral dust aerosol, Geophysical Research Letters, 32, 2005.
Zender, C. S., Bian, H., and Newman, D.: Mineral Dust Entrainment and Deposition (DEAD) model: Description and 1990s dust climatology, Journal of Geophysical Research: Atmospheres, 108, 2003.
Zeng, X., Shaikh, M., Dai, Y., Dickinson, R. E., and Myneni, R.: Coupling of the common land model to the NCAR community climate model, Journal of Climate, 15, 1832-1854, 2002.

687

Figures and tables

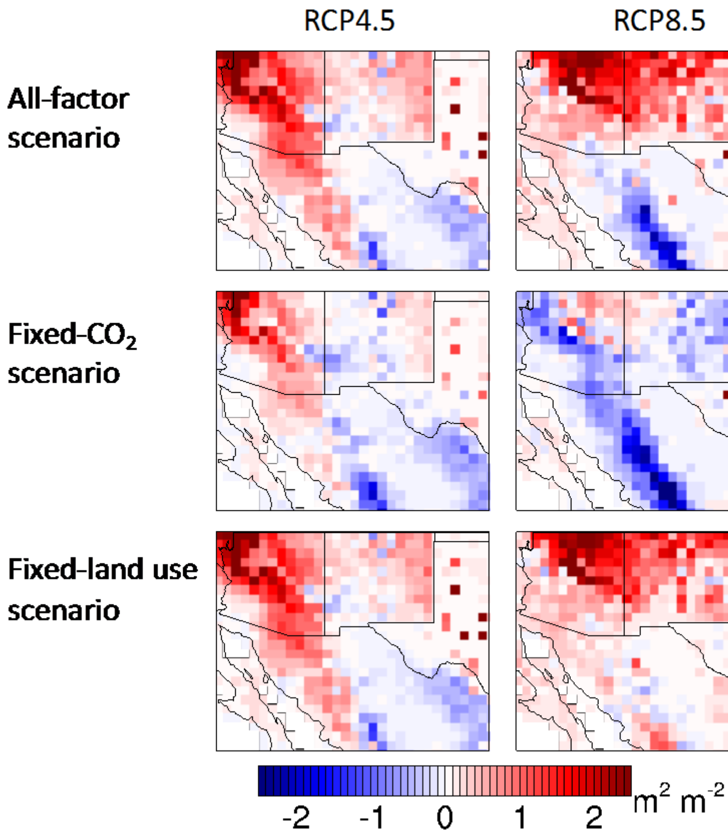

Figure 1. Simulated changes in spring averaged monthly mean vegetation area index (VAI) in southwestern North America under the three conditions for RCP4.5 and RCP8.5. Changes are between the present day and 2100, with five years representing each time period. The All-factor case (top row) includes the effects of climate, CO_2 fertilization, and land use on vegetation. Only climate and land use are considered in the Fixed-CO_2 case (middle), and only climate and CO_2 fertilization are considered in the Fixed-land use case (bottom). Results are from LPJ-LMfire.

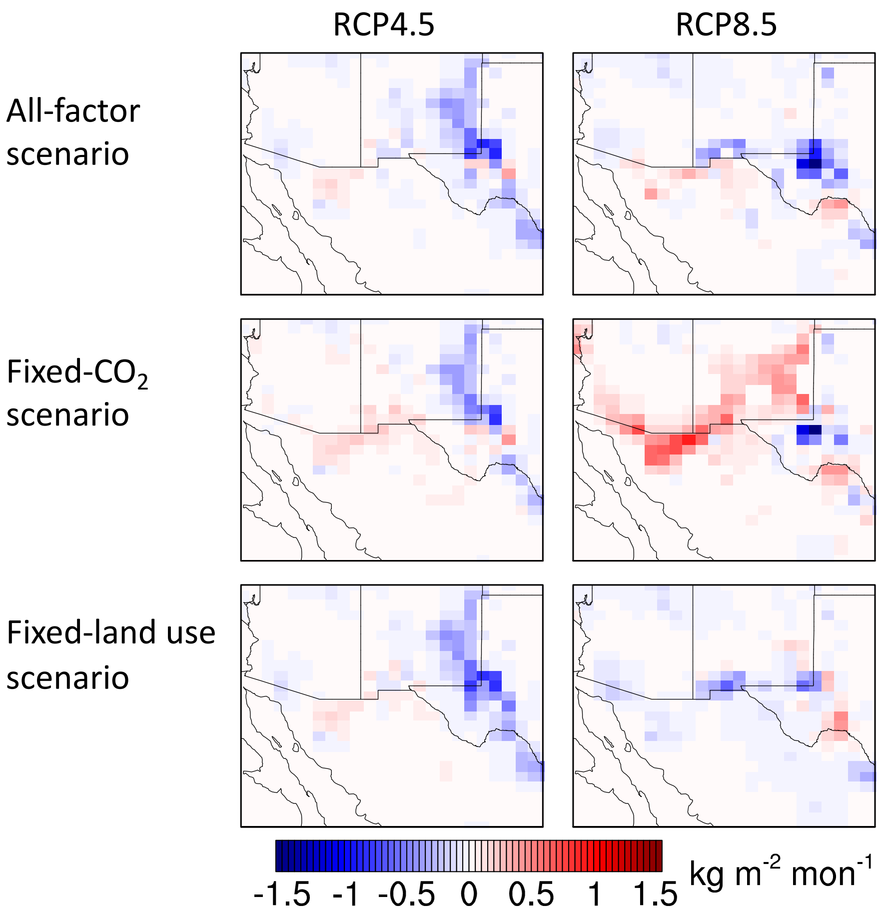

Figure 2. Simulated changes in spring averaged monthly mean dust emission in southwestern North America under the three conditions for RCP4.5 and RCP8.5. Changes are between the present day and 2100, with five years representing each time period. The top row shows results for the all-factor condition, the middle row is for the fixed-CO_2 condition, and the bottom row is for the fixed-land use condition. Cases are as described in Figure 1. Results are generated offline using the GEOS-Chem emission component (HEMCO).

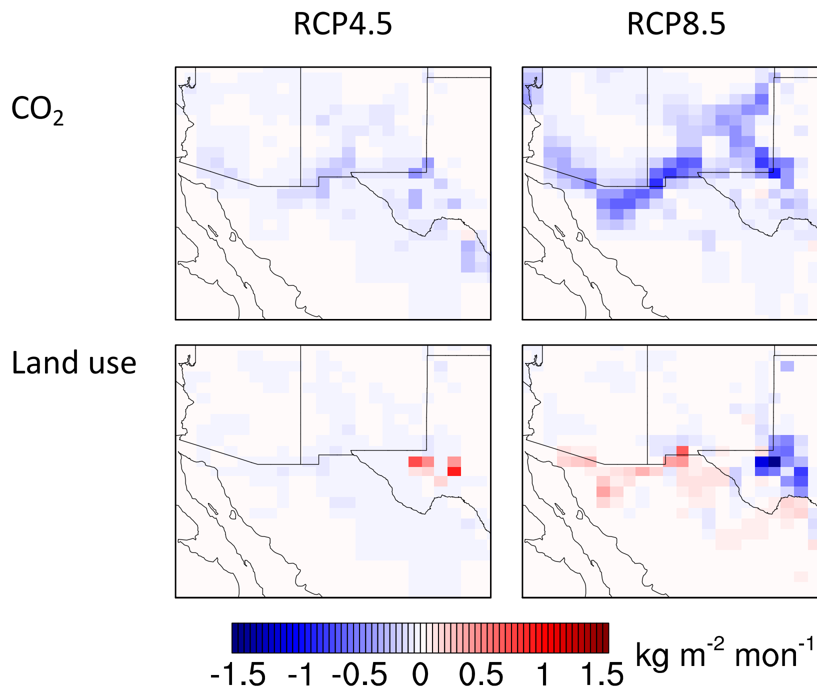

Figure 3. Contributions of CO_2 fertilization and land use change to changing dust emissions in spring in southwestern North America for RCP4.5 and RCP8.5. Changes are between the present day and 2100, with five years representing each time period. The top row shows the response of dust emission to only CO_2 fertilization and the bottom row shows the response to only trends in land use. Results are generated offline using the GEOS-Chem emission component (HEMCO).

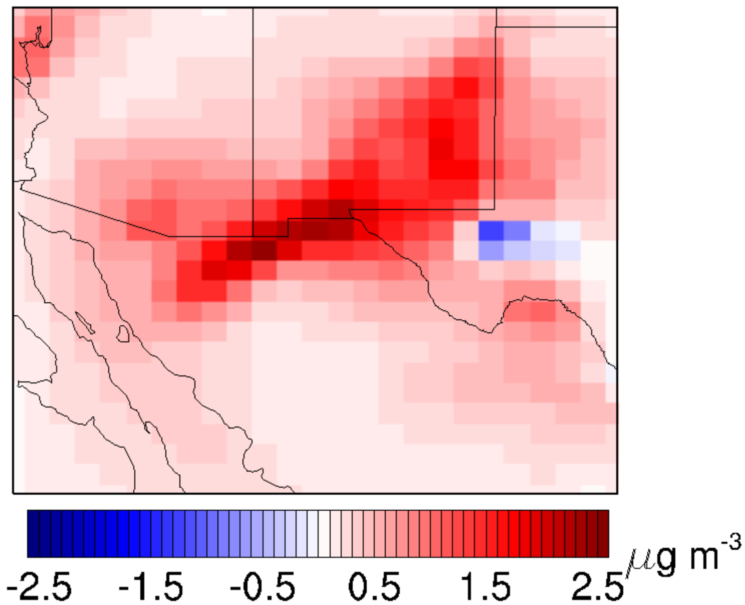

Figure 4. Simulated changes in springtime mean concentrations of fine dust over southwestern North America for the RCP8.5 fixed-CO_2 case, in which the effects of CO_2 fertilization are neglected. Changes are between the present day and 2100, with five years representing each time period. Results are from GEOS-Chem simulations at 0.5° x 0.625° resolution.

Table 1. Averaged spring vegetation area index (VAI) and fine dust emission in southwestern North America for the present-day and future for two scenarios (RCP4.5 and RCP8.5) and three cases. The all-factor case includes changes in climate, land use, and CO_2 fertilization; the fixed-CO_2 case includes changes in only climate and land use; and the fixed-land use case includes changes in only climate and CO_2. The rows labeled “2100-2010, %” give the percentage changes in VAI and fine dust emissions between the present day and future, with positive values denoting increases in the future.

		VAI[b], m^2 m^{-2}			**Fine dust emission[b], kg m^{-2} mon^{-1}**		
		All-factor	**Fixed CO_2**	**Fixed land use**	**All-factor**	**Fixed CO_2**	**Fixed land use**
RCP4.5	**2010[a]**	0.75±0.26	0.71±0.24	0.75±0.26	0.10±0.07	0.11±0.08	0.10±0.07
	2100[a]	1.07±0.48	0.79±0.34	1.07±0.48	0.08±0.04	0.10±0.05	0.08±0.04
2100-2010, %		**42**	**12**	**42**	**-25**	**-4**	**-26**
RCP8.5	**2010[a]**	0.80±0.27	0.75±0.24	0.75±0.24	0.09±0.04	0.09±0.05	0.09±0.04
	2100[a]	1.11±0.71	0.55±0.33	0.55±0.33	0.07±0.04	0.14±0.09	0.07±0.06
2100-2010, %		**38**	**-26**	**52**	**-20**	**58**	**-16**

[a]Each time slice represents 5 years (i.e., 2011-2015 represents the 2010 time slice and 2095-2099 represents the 2100 time slice); [b]Values are spring (MAM) averages over southwestern North America.